ACS Infectious Diseases

Letter

Cite This: ACS Infect. Dis. XXXX, XXX, XXX-XXX

pubs.acs.org/journal/aidcbc

Rigid Oxazole Acinetobactin Analog Blocks Siderophore Cycling in *Acinetobacter baumannii*

Tabbetha J. Bohac,‡ Justin A. Shapiro,‡ and Timothy A. Wencewicz*

Department of Chemistry, Washington University in St. Louis, One Brookings Drive, St. Louis, Missouri 63130, United States

Supporting Information

ABSTRACT: The emergence of multidrug resistant (MDR) Gram-negative bacterial pathogens has raised global concern. Nontraditional therapeutic strategies, including antivirulence approaches, are gaining traction as a means of applying less selective pressure for resistance *in vivo*. Here, we show that rigidifying the structure of the siderophore preacinetobactin from MDR *Acinetobacter baumannii* via oxidation of the phenolate-oxazoline moiety to a phenolate-oxazole results in a potent inhibitor of siderophore transport and imparts a bacteriostatic effect at low micromolar concentrations under infection-like conditions.

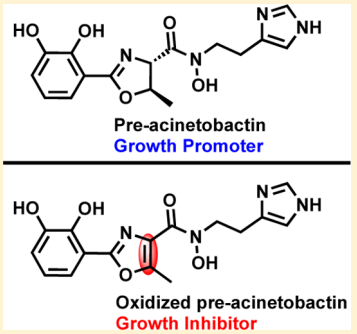

KEYWORDS: *antibiotic resistance, iron acquisition, antivirulence agent, metal chelation, metal transport, metal homeostasis, siderophore, pathogenesis, virulence*

The Centers for Disease Control and Prevention (CDC) and the World Health Organization (WHO) have identified multidrug resistant (MDR) bacterial pathogens as a serious global threat to human health.[1] Infections from MDR Gram-negative bacteria, including MDR *Acinetobacter baumannii*, are on the rise and are extremely difficult to cure. More than 63% of all health-care associated *A. baumannii* infections (~7000 annually) show resistance to three or more clinical antibiotic classes and result in 500 deaths annually in the United States.[1] The ineffectiveness of traditional antibiotics has inspired drug discovery efforts in nontraditional therapeutic areas including antivirulence strategies.[2,3] Unlike traditional antibiotics, antivirulence agents apply less selective pressure for resistance by targeting virulence factors that are only required for proliferation within the host.[4] *A. baumannii* produces virulence factors for nutrient acquisition,[5] biofilm formation,[6] cell adhesion,[7] and protein secretion[8] to establish infection. Iron is critical for all bacterial pathogens.[9] Proteins and effectors involved in iron acquisition are attractive antivirulence targets.[10]

A. baumannii relies primarily on a combination of siderophores, small-molecule iron(III) chelators, to solubilize iron(III) from the local infection environment. Pathogenic strains of *A. baumannii* typically biosynthesize a combination of three siderophores including the fimsbactins,[11] baumannoferrins,[12] and preacinetobactin[13] (PreAcb, **1**) (Figure 1). Murine infection models have shown that PreAcb is a virulence factor for *A. baumannii*.[14] Inhibitors of BasE, an adenylation domain for 2,3-dihydroxybenzoic acid (2,3-DHB) in the PreAcb nonribosomal peptide synthetase (NRPS), have been studied extensively as a method to block siderophore biosynthesis in *A. baumannii*.[15] Siderophore biosynthesis inhibitors have shown some efficacy *in vivo*,[16] but cell permeability and pharmacokinetics require improvement.[15] Alternative antivirulence strategies targeting siderophore-mediated iron acquisition include inhibition of TonB,[17] antibiotic delivery with siderophore-antibiotic conjugates (SACs),[18] siderophore sequestration with antibodies and siderocalins,[19] and disruption of siderophore cycling with competitive siderophore analogs.[20]

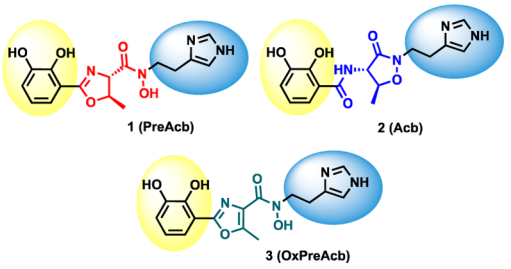

Figure 1. Structures of preacinetobactin (**1**), acinetobactin (**2**), and oxidized preacinetobactin (**3**).

Our laboratory seeks to understand the PreAcb pathway in great molecular detail.[21] The PreAcb pathway starts when the siderophore scaffold is assembled on an NRPS biosynthetic template.[22] After formation of the phenolate oxazoline moiety, the penultimate thioester is cleaved from the NRPS peptidylcarrier domain by *N*-hydroxyhistamine releasing PreAcb (**1**). Upon release from the NRPS, PreAcb is effluxed to the extracellular space where it isomerizes to the isooxazolidinone acinetobactin (Acb, **2**) (Figure 1).[22] The 5-*exotet* cyclization proceeds with clean stereochemical inversion

Received: September 6, 2017
Published: October 9, 2017

DOI: 10.1021/acsinfecdis.7b00146
ACS Infect. Dis. XXXX, XXX, XXX−XXX

at C5′ and shows a distinct pH-rate profile.[21] The isomzerization is slow at acidic pH and fast at neutral and basic pH. Both forms of the siderophore, **1** and **2**, promote the growth of *A. baumannii* ATCC 17978 under iron-restrictive conditions and use the same transport proteins. Given that most sites of *A. baumannii* infection are acidic, we hypothesize that both PreAcb and Acb will be present and functional as iron-sequestering virulence factors, providing a growth advantage under an expanded pH range. Consistent with this hypothesis, PreAcb accumulates in *A. baummannii* supernatants in acidic media, while only Acb is detectable in neutral media. Both PreAcb and Acb form stable, 2:1 complexes with iron(III). Structure−function studies of PreAcb and Acb analogs showed that iron(III) chelation is required for growth promotion of *A. baumannii* in iron-restrictive media.[23] Structural analogs incapable of promoting growth might competitively inhibit the Acb pathway.

Subtle structural changes in a siderophore scaffold can dramatically influence function. A single carbon epimer of mycobactin was shown to block siderophore cycling in *M. tuberculosis* leading to high intracellular accumlulation of siderophores that induced a lethal phenotype.[24] Mutasynthesis of pyochelin analogs by feeding substituted salicylate precursors to *P. aeruginosa* decreases the efficiency of iron uptake.[25] The modified pyochelin analogs are potential competitive inhibitors that block pyochelin uptake. Furthermore, oxidation of the thiazoline in pyochelin to the corresponding aromatic thiazole was shown to block transport of ferric pyochelin in *P. aeruginosa*.[26] Oxidized *des*-methyl pyochelin binds tightly to the pyochelin outer membrane transporter FptA and blocks uptake, but not binding, of ferric pyochelin. Computational docking and molecular dynamics simulations showed that oxidized pyochelin is more rigid than pyochelin, which might limit its ability to form stable metal complexes and increase stability of the FptA complex. The *des*-methyl phenolate-bis-thiazoline precursor to pyochelin is also a known intermediate in yersiniabactin biosynthesis.[27] Recently, Henderson and co-workers showed that yersiniabactin-producing Enterobacteriaceae also excrete oxidized *des*-methyl pyochelin, a compound now identified as escherichelin, to block virulence of opportunistic *P. aeruginosa* during clinical bacteriuria.[28] Escherichelin-producing Enterobacteriaceae have potential as probiotic treatments for urinary tract infections, and purified escherichelin might also be useful as an antivirulence agent. Similar to escherichelin blocking siderophore transport in pyochelin-utilizing pathogens, we hypothesize that oxidation of the PreAcb oxazoline to the corresponding aromatic oxazole (**3**) might rigidify the siderophore backbone, block isomerization to Acb, and result in inhibition of PreAcb/Acb uptake (Figure 1).

The synthesis of oxidized preacinetobactin (OxPreAcb, **3**) commenced with two precursors, *N*-Boc-*O*-benzylhydroxyhistamine **6** and oxazole benzyl ester **8** (Scheme 1). Hydroxyhistamine **6** was synthesized starting from histamine, as previously reported.[21,29] Diazotization/halogenation of histamine dihydrochloride **4** with sulfuric acid and potassium bromide, followed by addition of sodium nitrite, provided the corresponding bromo- and chloro-ethylimidazoles **5** in 52% yield, as a ∼ 3:1 bromo-/chloro-mixture. S_N2 displacement of halo-mixture **5** with the sodium salt of *N*-boc-*O*-benzylhydroxamine afforded *N*-Boc-*O*-benzylhydroxy-histame **6** in good yield. Oxazole **8** was synthesized in a one-pot, two-step synthesis adapted from Graham,[30] via the condensation of 2,3-

Scheme 1. Synthesis of Precursors to OxPreAcb (3)

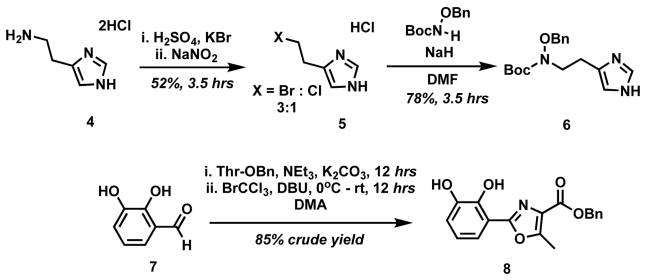

dihydroxybenzyaldehyde with Bn-protected L-Thr and subsequent oxidation of the intermediate aminal with $BrCCl_3$. Hydrogenolytic debenzylation of **8** and TFA-mediated Boc-removal of **6** generated the free acid **9** and amine **10**, respectively (Scheme 2). EDC/HOBt coupling of **9** and **10**

Scheme 2. Synthesis of OxPreAcb (3)

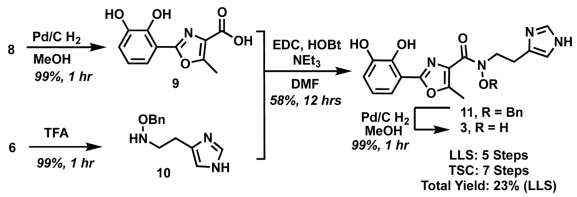

provided *O*-benzyl protected *N*-hydroxyamide **11**. Hydrogenolysis of **11** yielded OxPreAcb **3** to complete the synthesis in the 5 longest linear steps (LLS) and 7 total steps.

OxPreAcb is stable and does not spontaneously isomerize in aqueous buffer as observed for the oxazoline to isooxazolidinone isomerization from PreAcb and Acb.[21] Thus, OxPreAcb is structurally "locked" in the PreAcb-like form via aromatization to the phenolate-oxazole heterocycle. We investigated the effect of Acb and OxPreAcb on the growth of *A. baumannii* ATCC 19606T in M9 minimal medium under iron-restrictive (125 μM 2,2′-dipyridyl) conditions. We chose Acb over PreAcb because we have shown in previous work that both isomers have equivalent growth promoting effects at pH 7 and Acb is easier to isolate from *A. baumannii* cultures.[21] As expected, Acb promoted the growth of *A. baumannii* ATCC 19606T in a dose-dependent manner (Figure 2A). In striking contrast, OxPreAcb strongly inhibited growth at all concentrations tested (0.78−50 μM) (Figure 2B). Furthermore, growth inhibition by OxPreA was competitive and dose dependent in the presence of 10 μM Acb (Figure 2C). Antagonism of OxPreAcb growth inhibitory activity by Acb supports competition for the same biological target or transport pathway. OxPreAcb activity was confirmed on two separate synthetic lots to confirm the observed biological activity (Supplementary Figure S1). In medium supplemented with 100 μM 2,2′-dipyridyl, OxPreAcb inhibited *A. baumannii* ATCC 19606T growth with an MIC of 1.56 μM.

To probe the iron dependence of OxPreAcb activity, wild-type *A. baumannii* ATCC 19606T and a biosynthesis deficient ATCC 19606T s1 mutant were grown in M9 media in the presence of variable OxPreAcb with and without supplemented 10 μM $Fe(acac)_3$ (Figure 3). Ciprofloxacin was included as a control antibiotic with activity that is not strongly affected by iron concentration.[31] As expected, ciprofloxacin activity against *A. baumannii* ATCC 19606T and the s1 mutant was not affected by iron concentration. However, the growth inhibitory

DOI: 10.1021/acsinfecdis.7b00146
ACS Infect. Dis. XXXX, XXX, XXX−XXX

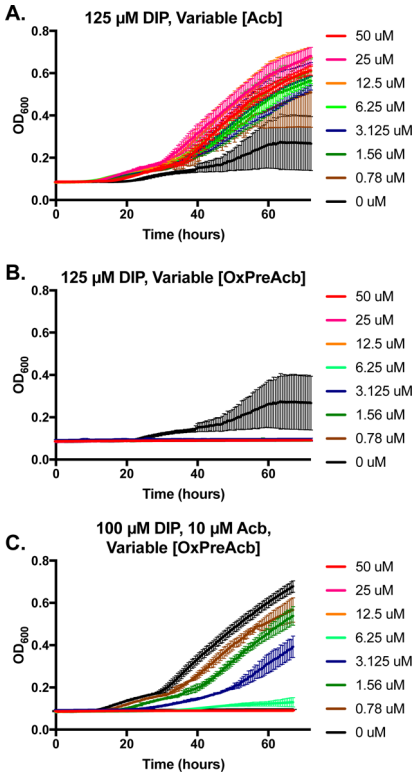

Figure 2. OxPreAcb (**3**) competes with Acb (**2**) to inhibit *A. baumannii* growth. Growth curves of *A. baumannii* ATCC 19606T in M9 minimal medium supplemented with 125 μM 2,2′-dipyridyl (DIP) and gradient concentrations of Acb (A), 125 μM DIP and gradient concentrations of OxPreAcb (B), and 100 μM DIP, 10 μM Acb, and gradient concentrations of OxPreAcb (C). Error bars represent s.d. for three independent trials.

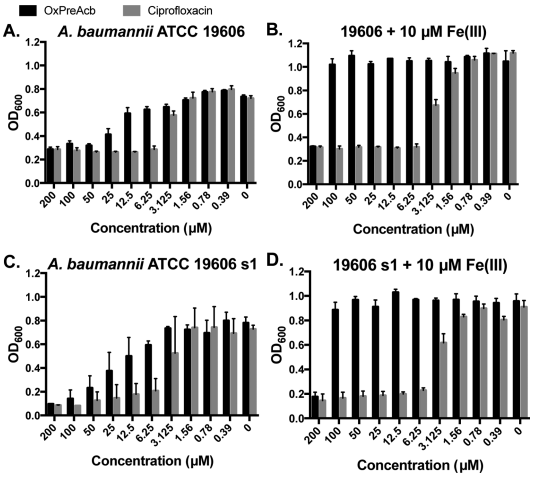

Figure 3. Growth inhibition by OxPreAcb (**3**) is attenuated by iron. OD_{600} taken at 42 h of *A. baumannii* ATCC 19606T and 19606T s1 (Acb biosynthesis mutant) grown in M9 minimal medium supplemented with gradient concentrations of either OxPreAcb (**3**) (black bars) or ciprofloxacin (gray bars). No DIP was added to the media. (A) Wild-type *A. baumannii* ATCC 19606T. (B) Wild-type ATCC 19606T supplemented with 10 μM $Fe(acac)_3$. (C) ATCC 19606T s1. (D) ATCC 19606T s1 supplemented with 10 μM $Fe(acac)_3$. Error bars represent s.d. for three independent trials.

activity of OxPreAcb was strongly antagonized by iron supplementation. The amount of OxPreAcb required to fully inhibit growth of wild-type ATCC 19606T and ATCC 19606T s1 was 50 μM (Figure 3A,C). Upon supplementation with 10 μM $Fe(acac)_3$, the concentration of OxPreAcb required to fully inhibit growth increased to 200 μM (Figure 3B,D). PreAcb biosynthesis is under the transcriptional control of ferric uptake repressors (FURs).[22] FUR proteins repress transcription when bound to Fe(II) and allow transcription when no metal is bound. This level of transcriptional control ensures that expression of proteins in costly siderophore pathways remains reserved for times of iron restriction when the metal is needed most. Iron dependence is commonly observed for SACs and other antibiotics that rely on siderophore-binding proteins for cell entry.[32] Thus, OxPreAcb might be entering cells via the Acb pathway.

To investigate the role of Acb transport proteins on the growth inhibiting activity of OxPreAcb, we performed growth studies in M9 medium using gene insertion mutants of *A. baumannii* ATCC 19606T t6 and t7, which are deficient in the outer membrane receptor protein BauA and inner-membrane transport protein BauD, respectively (Supplementary Figure 2).[21] Wild-type ATCC 19606T and the t7 mutant showed similar levels of growth, while the s1 and t6 mutants showed reduced growth across multiple concentrations of OxPreAcb (Supplementary Figure 2A). Interestingly, when OxPreAcb was precomplexed with iron(III) prior to growth studies, the growth of wild-type *A. baumannii* ATCC 19606T and the s1, t6, and t7 mutants was promoted suggesting that the OxPreAcb-iron(III) complex can be used as a source of iron and only the metal-free form of OxPreAcb has growth inhibitory activity (Supplementary Figure 2B). Disrupting Acb biosynthesis and transport systems does not strongly affect the growth inhibitory activity of OxPreAcb. The activity of OxPreAcb is antagonized by supplementing growth medium with iron(III). Thus, it remains unclear whether complexation of OxPreAcb truly abolishes the growth inhibitory effect or if that added iron(III) is simply having the same antagonistic effect as supplementation with $Fe(acac)_3$. During human infections, iron is a limiting nutrient so OxPreAcb would presumably be metal free and growth inhibitory toward *A. baumannii* pathogens.[5] The overall growth inhibitory effect of OxPreAcb on *A. baumannii* appears to be bacteriostatic (Supplementary Figure 3).

We tested the antibiotic activity of OxPreAcb against two additional clinical isolates of *A. baumannii* (ATCC 17978 and ATCC 19961), the nonpathogenic strain *Acinetobacter baylyi* ATCC 33305, and pathogenic *E. coli* ATCC 29522 (Supplementary Figure 4). The iron-restrictive M9 medium supplemented with DIP was optimized specifically for *A. baumannii* ATCC 19606T. To ensure growth of all the strains, the M9 media was not supplemented with DIP, which reduces the potency of OxPreAcb for inhibiting bacterial growth (similar to supplementing $Fe(acac)_3$). OxPreAcb inhibited the growth of all the Gram-negative bacteria at 100−200 μM. This could indicate that a more general mechanism than siderophore disruption, such as metal withholding or metalloenzyme targeting, is at play. All of the *Acinetobacter* strains produce Acb, and *E. coli* is known to transport catecholate siderophores, so a siderophore-based inhibition mechanism is still possible.

The conversion of OxPreAcb from a growth inhibitor to a growth promoter upon iron(III) chelation inspired us to study the iron(III) binding properties. We used a fluorescence quenching assay to titrate OxPreAcb with iron(III) showing

DOI: 10.1021/acsinfecdis.7b00146
ACS Infect. Dis. XXXX, XXX, XXX−XXX

that a stable 2:1 $(OxPreAcb)_2Fe(III)$ complex forms (Supplementary Figure 5). PreAcb and Acb also form stable 2:1 complexes with iron(III).[23] We used an EDTA competition assay to measure the apparent stability constants (K_{Fe}) of the $(PreAcb)_2Fe(III)$, $(Acb)_2Fe(III)$, and $(OxPreAcb)_2Fe(III)$ complexes (Supplementary Figure 6). Apparent K_{Fe} values were 27.4 ± 0.2, 26.2 ± 0.1, and 26.5 ± 0.3 for $(PreAcb)_2Fe(III)$, $(Acb)_2Fe(III)$, and $(OxPreAcb)_2Fe(III)$, respectively. On the basis of the similarity of the apparent K_{Fe} values, we predict that OxPreAcb will be competitive with PreAcb and Acb for iron(III) in a biological setting.

The mechanistic basis for the growth inhibitory activity of OxPreAcb against Gram-negative bacteria remains unknown. Simple oxidation of the PreAcb oxazoline to the OxPreAcb oxazole is predicted to increase rigidity of the siderophore backbone. Energy minimization of the metal-free PreAcb and OxPreAcb structures revealed significant differences in 3D-orientations of the phenolate-oxazoline and phenolate-oxazole moieties, respectively (Supplementary Figure 7). Both the phenolate-oxazoline and phenolate-oxazole systems are relatively flat, with the *trans*-oxazoline of PreAcb slightly puckered and the oxazole of OxPreAcb appearing in plane with the phenyl ring. In the gas phase, a stable H-bond was predicted between the 2-hydroxyl group of the phenyl ring with the oxazoline nitrogen of PreAcb, which presumably stabilizes the planar structure and restricts rotation around the oxazoline C1 to phenyl C1′ bond. The same type of H-bonding interaction was found in the OxPreAcb energy minimized structure except the H-bond was formed between the oxazole nitrogen and the hydroxyl group of the hydroxamic acid. PreAcb is capable of this same H-bonding interaction, but it was not found during energy minimization. The origin for this difference in H-bonding modes might be the relative rotational barriers about the oxazoline/oxazole C4 to hydroxamate carbonyl carbon bond. The *trans*-orientation of the oxazoline methyl and hydroxamate substituents decreases steric clash in rotational isomers. The *cis*-planar orientation of the oxazole methyl and hydroxamate substituents introduces $A_{1,3}$-strain. Computational analysis of the energy landscape for rotational isomers about the oxazoline/oxazole C4 to hydroxamate carbonyl carbon bond of PreAcb and OxPreAcb supported this model (Figure 4; Supplementary Figure 8). The sterically smaller carbonyl group of the hydroxamate prefers to eclipse the oxazole methyl group to minimize the $A_{1,3}$-strain, which puts the bulky *N*-alkyl-*N*-hydroxy group closer to the oxazole nitrogen. Restricted rotation in the rigid phenolate-oxazole ligand set of OxPreAcb is predicted to limit the accessible number of theoretical modes for iron(III) chelation compared to the more flexible PreAcb and Acb structures. In medicinal chemistry, rigidity is often used to increase the affinity of a ligand for a protein target.[33] Escherichelin, a rigid pyochelin analog, was shown to tightly bind the outer membrane receptor FptA and block transport of ferric pyochelin.[26] A similar phenomenon might be taking place in *A. baumannii* for OxPreAcb in the presence of Acb. Like escherichelin,[28] OxPreAcb might be effective at blocking virulence of *A. baumannii* by disrupting siderophore utilization, which is required for growth during infection (Supplementary Figure 9).[14] Here, the importance of molecular recognition is revealed by subtle structural changes (Supplementary Figure 10). A more detailed understanding of siderophore receptor binding and membrane transport paradigms in *A. baumannii* is required to fully appreciate how OxPreAcb competes with Acb for cellular uptake.[34] It also remains unclear whether the net growth inhibitory effect of OxPreAcb is due exclusively to blocking siderophore cycling or if inhibition of metalloenzymes or disruption of metal homeostasis are contributing factors.[35] Phenolate-oxazolines and phenolate-thiazolines are common motifs in many siderophore scaffolds, including siderophores associated with virulence in bacterial pathogens.[36] Simple oxidation of the oxazolines/thiazolines found in bacterial siderophores might be a general strategy for preparing rigid siderophore analogs as antivirulence agents that competitively block siderophore utilizaton in producing pathogens.

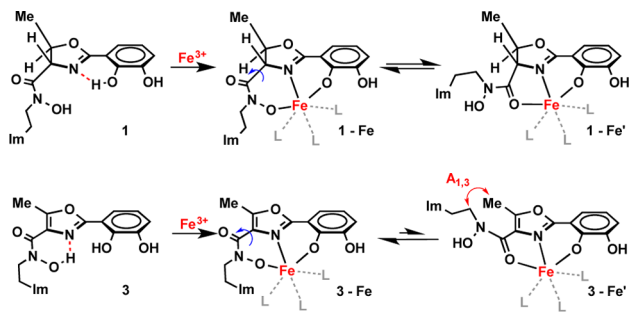

Figure 4. $A_{1,3}$-strain induces conformational rigidity. Energy minimization shows OxPreAcb adopts a planar geometry causing reduced flexibility, which may contribute to antibiotic properties.

■ ASSOCIATED CONTENT

Supporting Information

The Supporting Information is available free of charge on the ACS Publications website at DOI: 10.1021/acsinfecdis.7b00146.

Experimental details, spectroscopic data of new compounds, and additional data/figures (PDF)

■ AUTHOR INFORMATION

Corresponding Author

*E-mail: wencewicz@wustl.edu.

ORCID

Timothy A. Wencewicz: 0000-0002-5839-6672

Author Contributions

‡T.J.B. and J.A.S. contributed equally to this work.

Notes

The authors declare no competing financial interest.

■ ACKNOWLEDGMENTS

We thank Drs. Jeff Kao and Manmillan Singh (WUSTL) for help with 2D NMR and Dr. Brad Evans (Danforth Plant Science Center, NSF DBI-0521250) for acquisition of HRMS. Research was supported by NSF CAREER Award 1654611 to T.A.W.

■ REFERENCES

(1) CDC. (2013) *Antibiotic Resistance Threats in the United States, 2013*, Centers for Disease Control and Prevention, U.S. Department of Health and Human Services, Washington D.C.

(2) Mühlen, S., and Dersch, P. (2015) *Curr. Top. Microbiol. Immunol. 398*, 147−183.

(3) Dickey, S. W., Cheung, G., and Otto, M. (2017) *Nat. Rev. Drug Discovery 16*, 457−471.

(4) Allen, R. C., Popat, R., Diggle, S. P., and Brown, S. P. (2014) *Nat. Rev. Microbiol. 12*, 300−308.

DOI: 10.1021/acsinfecdis.7b00146
ACS Infect. Dis. XXXX, XXX, XXX−XXX

(5) Mortensen, B. L., and Skaar, E. P. (2013) *Front. Cell. Infect. Microbiol. 3*, 95.
(6) Gaddy, J. A., and Actis, L. A. (2009) *Future Microbiol. 4*, 273−278.
(7) Smani, Y., McConnell, M. J., and Pachón, J. (2012) *PLoS One 7*, e33073.
(8) Carruthers, M. D., Nicholson, P. A., Tracy, E. N., and Munson, R. S., Jr. (2013) *PLoS One 8* (3), e59388.
(9) Payne, S. M., and Finkelstein, R. A. (1978) *J. Clin. Invest. 61*, 1428−1440.
(10) Foley, T. L., and Simeonov, A. (2012) *Expert Opin. Drug Discovery 7*, 831−847.
(11) Proschak, A., Lubuta, P., Grün, P., Löhr, F., Wilharm, G., De Berardinis, V., and Bode, H. B. (2013) *ChemBioChem 14*, 633−8.
(12) Penwell, W. F., DeGrace, N., Tentarelli, S., Gauthier, L., Gilbert, C. M., Arivett, B. A., Miller, A. A., Durand-Reville, T. F., Joubran, C., and Actis, L. A. (2015) *ChemBioChem 16*, 1896−1904.
(13) Yamamoto, S., Okujo, N., and Sakakibara, Y. (1994) *Arch. Microbiol. 162*, 249−54.
(14) Gaddy, J. A., Arivett, B. A., McConnell, M. J., López-Rojas, R., Pachón, J., and Actis, L. A. (2012) *Infect. Immun. 80*, 1015−24.
(15) Neres, J., Engelhart, C. A., Drake, E. J., Wilson, D. J., Fu, P., Boshoff, H. I., Barry, C. E., Gulick, A. M., and Aldrich, C. C. (2013) *J. Med. Chem. 56*, 2385−2405.
(16) Lun, S., Guo, H., Adamson, J., Cisar, J. S., Davis, T. D., Chavadi, S. S., Warren, J. D., Quadri, L. E., Tan, D. S., and Bishai, W. R. (2013) *Antimicrob. Agents Chemother. 57*, 5138−5140.
(17) Yep, A., McQuade, T., Kirchhoff, P., Larsen, M., and Mobley, H. L. (2014) *mBio 5* (2), e01089-13.
(18) Wencewicz, T. A., and Miller, M. J. (2013) *J. Med. Chem. 56*, 4044−52.
(19) Correnti, C., Clifton, M. C., Abergel, R. J., Allred, B., Hoette, T. M., Ruiz, M., Cancedda, R., Raymond, K. N., Descalzi, F., and Strong, R. K. (2011) *Structure 19*, 1796−1806.
(20) Miethke, M., and Marahiel, M. A. (2007) *Microbiol. Mol. Biol. Rev. 71*, 413−451.
(21) Shapiro, J. A., and Wencewicz, T. A. (2016) *ACS Infect. Dis. 2*, 157−168.
(22) Wuest, W. M., Sattely, E. S., and Walsh, C. T. (2009) *J. Am. Chem. Soc. 131*, 5056−5057.
(23) (a) Shapiro, J. A., and Wencewicz, T. A. (2017) *Metallomics 9*, 463−470. (b) Song, W. Y., Jeong, D., Kim, J., Lee, M. W., Oh, M. H., and Kim, K. J. (2017) *Org. Lett. 19*, 500−503. (c) Balado, M., Segade, Y., Rey, D., Osorio, C. R., Rodriguez, J., Lemos, M. L., and Jiménez, C. (2017) *ACS Chem. Biol. 12*, 479−493.
(24) Liu, Z., Liu, F., and Aldrich, A. (2015) *J. Org. Chem. 80*, 6545−6552.
(25) Mislin, G., Burger, A., and Abdallah, M. (2004) *Tetrahedron 60*, 12139−12145.
(26) Mislin, G., Hoegy, F., Cobessi, D., Poole, K., Rognan, D., and Schalk, I. (2006) *J. Mol. Biol. 357*, 1437−1448.
(27) Miller, D. A., Luo, L., Hillson, N., Keating, T. A., and Walsh, C. T. (2002) *Chem. Biol. 9*, 333−344.
(28) Ohlemacher, S. I., Giblin, D. E., d'Avignon, D. A., Stapleton, A. E., Trautner, B. W., and Henderson, J. P. (2017) *J. Clin. Invest.*, Epub ahead of print, DOI: 10.1172/JCI92464.
(29) Takeuchi, Y., Ozaki, S., Satoh, M., Mimura, K., Hara, S., Abe, H., Nishioka, H., and Harayama, T. (2010) *Chem. Pharm. Bull. 58*, 1552−1553.
(30) Graham, T. (2010) *Org. Lett. 12*, 3614−3617.
(31) Motoya, T., Miyashita, M., Kawachi, A., and Yamada, L. (2000) *J. Pharm. Pharmacol. 52*, 397−401.
(32) de Carvalho, C., and Fernandes, P. (2014) *Front. Microbiol. 5*, 1−3.
(33) Huggins, D., Sherman, W., and Tidor, B. (2012) *J. Med. Chem. 55*, 1424−1444.
(34) Stintzi, A., Barnes, C., Xu, J., and Raymond, K. N. (2000) *Proc. Natl. Acad. Sci. U. S. A. 97*, 10691−10696.
(35) Chan, A. N., Shiver, L. S., Wever, W. J., Razvi, S. Z. A., Traxler, M. F., and Li, B. (2017) *Proc. Natl. Acad. Sci. U. S. A. 114*, 2717−2722.
(36) Hider, R. C., and Kong, X. (2010) *Nat. Prod. Rep. 27*, 637−657.

DOI: 10.1021/acsinfecdis.7b00146
ACS Infect. Dis. XXXX, XXX, XXX−XXX